SECRETORY KINETICS IN THE FOLLICULAR CELLS OF SILKMOTHS DURING EGGSHELL FORMATION

HELEN M. BLAU and FOTIS C. KAFATOS

From the Biological Laboratories, Harvard University, Cambridge, Massachusetts 02138. Dr. Blau's present address is the Department of Pharmacology, Stanford University, Stanford, California 94305.

ABSTRACT

Procedures for quantitative autoradiography were used for studying the process of secretion of eggshell (chorion) proteins in the follicular epithelium of silkmoths. The method was based on photometric measurements of the reflectance of vertically illuminated autoradiographic silver grains. Results were analyzed and plotted by computer. Secretory kinetics were also determined by analysis of labeled proteins in physically separated epithelium and chorion. Rapid accumulation of radioactivity into "clumps" visualized by light microscope autoradiography and evidence from preliminary electron microscope autoradiography indicate that, within 2 min from the time of synthesis, labeled chorion proteins move to Golgi regions scattered throughout the cytoplasm. The proteins begin to accumulate in the apical area 10–20 min later and to be discharged from the cell. The time for half-secretion is 20–25 min, and discharge is essentially complete 30–50 min after labeling. At the developmental stages examined, the kinetics of secretion appear to be similar for all proteins. Within the chorion the proteins rapidly assume a characteristic distribution, which varies for different developmental stages. Two relatively slow steps have been identified in secretion, associated with residence in Golgi regions and in the cell apex, respectively. By contrast, translocation of proteins across the cell and deposition of discharged proteins in the chorion are rapid steps.

KEY WORDS secretion · kinetics · quantitative autoradiography · photometry · intracellular transport

Kinetic studies of the secretory pathway have been limited by the methods commonly used, subcellular fractionation and electron microscopic autoradiography. These methods are well suited for identifying the organelles involved but are somewhat cumbersome for detailed kinetic studies. In the present paper, we describe widely applicable methods for quantitative light microscopic autoradiography. These methods have expedited the quantitative analysis of large numbers of autoradiograms, making possible detailed studies of secretory kinetics in the follicular epithelium of silkmoths. Studies using separation of cells from extracellular secreted products, plus preliminary electron microscope autoradiography, corroborated and extended the results of light microscope autoradiography. The major steps involved in secretion were identified and the duration of each step was evaluated.

The follicular epithelium is well suited for studying secretory kinetics. It forms a monolayer around each oocyte and during the terminal pe-

riod of oogenesis produces and secretes massive amounts of structural proteins to form the protective eggshell or chorion (Fig. 1). During this period (choriogenesis), nearly all the proteins synthesized by the follicular cells are secretory chorion proteins (>95% of the incorporated glycine); thus secretion can be studied by autoradiography against a very low background of nonsecretory proteins. Secretion is strictly limited to the apical cell surface, and the secreted proteins are immobilized within the chorion, adjacent to the secretory cells, permitting quantitative assessment of the proteins even after secretion. The follicular cells are terminally differentiated: they secrete a specific set of products over a defined period and then atrophy. Synthesis and secretion thus proceed without interruption, uncomplicated by storage adaptations and the external neural or humoral controls characteristic of cyclically active cells. The cells are active in organ culture, making possible the short pulse durations and effective chase incubations essential for studying kinetics. A series of developmental stages can be obtained conveniently, so that secretion can be studied for different proteins as a function of differentiation.

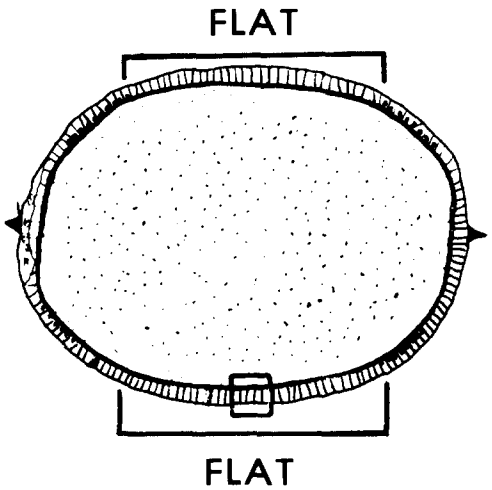

FIGURE 1 Diagram of a section of a choriogenic follicle of *A. polyphemus*. The follicle is oriented with the anterior end to the left. Thin strands at the anterior and posterior ends connect it to neighboring follicles (not shown; see Fig. 1 in reference 38). The yolky oocyte occupies most of the follicle and is surrounded by the chorion (dark line), which in turn is surrounded by the monolayer of secretory follicular epithelium. The two flat sides of the follicle studied in this report are indicated. Several follicular cells and the chorion they have secreted are outlined; cf. Fig. 3*a* and *b*.

MATERIALS AND METHODS

Dissection of Follicles, Organ Culture, and Labeling

Progressively more mature follicles are found interconnected in a linear array within each of the eight ovarioles of the developing silkmoth (25). Choriogenesis occurs within approximately 50 h at the end of follicle maturation, and is subdivided into 17 stages (Ia-Ie, II-IX, and Xa-Xd), defined by the changing profile of proteins synthesized (5, 26). Unless otherwise indicated, synthetic stages were determined for each labeled follicle by analyzing the newly synthesized proteins by sodium dodecyl sulfate (SDS)-polyacrylamide gel electrophoresis. Follicles can also be roughly staged according to their position within the ovariole (25). In this case, stages are designated by arabic numerals, relative to the end of vitellogenesis (position zero) and ovulation (the shedding of the follicular epithelium which usually occurs at position 12 ± 4). Although the absolute number of choriogenic follicles varies (even among the ovarioles of a single animal), if the ovariole is assumed to be in steady state, the fractional position of each chorion-producing follicle within the ovariole, between the end of vitellogenesis and ovulation, can be approximately correlated with the synthetic stage, as shown in Table I.

Follicles were dissected from developing *Antheraea polyphemus* pupae and incubated at 25°C in Grace's (9) tissue culture medium without hemolymph (GM). The follicles were labeled for 1-6 min in GM modified to contain reduced amounts of the amino acid used as tracer, rinsed thoroughly, and chased in normal GM (25, 26). The chase was effective, as shown by abrupt termination of incorporation after the pulse (5). The labeling conditions varied as follows: [^{3}H]glycine, 7.3-10.2 Ci/mmol, 0.25-4.0 mCi/ml, autoradiographic exposure 6-28 days; [^{3}H]leucine, 33.6-44.2 Ci/mmol, 0.25-3.0 mCi/ml, autoradiographic exposure 9-12 days. Radiochemicals were purchased from New England Nuclear, Boston, Mass. At the end of the chase, each follicle was cut to remove the yolk and either processed for microscopy and autoradiography or used for obtaining chorion and epithelium fractions by dissection.

Tissue Processing for Microscopy and Autoradiography

Tissues were fixed in 2% glutaraldehyde in 0.08 M phosphate buffer, pH 7.2, at room temperature and postfixed in 2% OsO_4 in 0.15 M phosphate buffer, pH 7.2, at 0°C; or they were fixed in 2.5% glutaraldehyde in 0.05 M sodium cacodylate – 0.03 M sucrose, pH 7.6, at room temperature and postfixed in 1% OsO_4 in 0.025 M sodium cacodylate – 0.03 M sucrose, pH 7.6, at room temperature. Tissues were embedded in Araldite, and 1-μm thick sections were cut and either stained or processed for autoradiography.

Conditions for quantitative autoradiography as de-

TABLE I

Correlation between Synthetic State and Fractional Position within the Ovariole

Synthetic stage	Fractional position			
	Estimate from equal duration	Estimate from observed duration	Estimate from observed frequency	Observed average position
0	0	0	0	0
Ia	0.06	0.06	0.05	0.08
Ib	0.11	0.12	0.14	0.15
Ic	0.17	0.18	0.18	0.24
Id	0.22	0.24	0.23	0.21
Ie	0.28	0.30	0.29	0.27
II	0.33	0.35	0.37	0.27
III	0.39	0.41	0.43	0.33
IV	0.44	0.46	0.49	0.42
V	0.50	0.51	0.56	0.43
VI	0.56	0.56	0.59	0.46
VII	0.61	0.61	0.64	0.51
VIII	0.67	0.66	0.69	0.52
IX	0.72	0.72	0.76	0.63
Xa	0.78	0.77	0.81	0.70
Xb	0.83	0.83	0.87	0.74
Xc	0.89	0.89	0.89	0.78
Xd	0.94	0.94	0.92	0.92
Ovulation	1.00	1.00	1.00	1.00

This correlation is based on raw data presented in reference 39. Follicles at position zero are invariably at synthetic stage zero, i.e., do not synthesize chorion proteins. By definition, the first post-ovulatory follicle is fractional position 1.00. The average fractional position of follicles at each synthetic stage of choriogenesis is estimated in four different ways. The estimates in the first three columns assume that ovarioles are at steady state, and are most dependable with healthy animals in the middle of chorion production (days 14–early 15 of adult development). The first column assumes that all stages have exactly equal durations, the second is based on the approx. equal stage durations determined experimentally, and the third assumes that the stage durations are reflected in the frequency of the stages in 124 follicles dissected from a number of animals. The last column reports the observed average absolute position of these staged follicles.

fined by Rogers (30, 31) were modified and standardized for our material (5) Liquid Ilford L4 nuclear track emulsion (Ilford Ltd., Ilford, Essex, England) was mixed 1:1 by weight with 1% glycerol at 42°C. Unstained sections affixed to thoroughly precleaned slides were dipped into emulsion, using a simplified Kopriwa dipping machine (20) at a constant rate of 10 cm/min. Safelight conditions (OC Wratten filter [Eastman Kodak Co.] and 7.5-W bulb) were maintained throughout, and coated slides were air-dried at room temperature in 40–50% humidity for at least 1 h. Slides were stored with desiccant at 4°C and then developed in Dektol (Eastman Kodak Co.) at 23°C for 3.0 or 3.5 min. Cover slips (Gold Seal thinness 0 [Clay-Adams, Div., Parsippany, N. J.]) were applied with Zeiss L15 (n_D 1.515) phase-contrast mounting medium (Carl Zeiss, Inc., New York). The choice of emulsion and developer and the conditions of dipping and drying yielded a sufficiently uniform layer of silver bromide crystals (5, 19, 22). The developed silver grains were adequate in size and density to give a significant photometric signal but small enough to avoid loss of resolution and loss of linearity at the most intensely labeled sites. The photometric response was linear over two orders of magnitude or grain density (Fig. 2). The mounting medium permitted good resolution by phase contrast so that staining, which resulted in unacceptable background reflectance, was unnecessary.

Photometry of Autoradiograms

The photometric method adopted for quantifying autoradiograms was based on the independent findings of Gullberg (11) and of Rogers (31, 32) that silver grains, when illuminated from above, reflect light in proportion to their number in a given area. The microscope used was a Leitz Ortholux MPV1. For vertical illumination, a high intensity sodium/mercury vapor light source (ST-75) was used, stabilized against voltage fluctuation. An adjustable diaphragm in front of the source controlled the size of the illuminated area. The beam of light was both projected downward onto the specimen and then reflected upward through the objective lens itself. To maximize the brightness of the image, an oil immersion lens of high numerical aperture (1.15) was

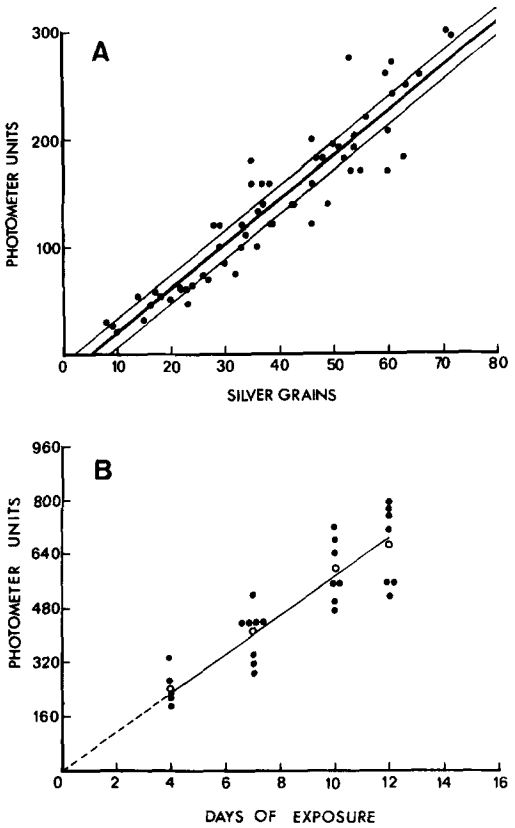

FIGURE 2 Linearity of the photometer response. (*A*) The silver grains in 60 randomly selected 50-μm^2 areas of follicular cell autoradiograms were counted manually and photometer readings were taken. The data plus a regression line with its standard error are plotted. Manual counting at high grain densities is inaccurate. (*B*) The linearity of the photometer at high grain densities was established using uniformly labeled sections. An ethanol solution of [^{3}H]leucine was evenly mixed with Araldite resin and a block was polymerized. Sections were exposed for autoradiography for 4–12 days. Photometric measurements of randomly selected 20-μm^2 areas (●) and averages (○) are plotted, together with the regression line.

selected. The reflected light passed through a measuring diaphragm and was then detected by a photometer (Photovolt Corp., New York; 520 M) connected to a strip chart recorder (Esterline Angus Instrument Corp., Indianapolis, Ind.).

A Heine condenser facilitated the interchange of phase-contrast and dark field illumination used for observing cellular morphology and grain distribution at a magnification of 25. For photometry, the × 70 vertical illumination objective was brought into operation. A potentially serious error, detection of stray or scattered light reflected by neighboring areas (Schwarzchild-Villiger effect [12]), was minimized by exactly superimposing illuminating and measuring diaphragms, so as to illuminate only that area which was measured.

Spatial Analysis of Silver Grain Distribution

Secretion (exocytosis) occurs at the border between cell and chorion. This boundary between secreted and nonsecreted products was the reference point for all measurements. Figs. 3 and 4*e* show that the border is distinct both in stained follicular preparations and in unstained preparations examined by phase microscopy. Fig. 3*a* also schematizes the progression of measurements across the cell and chorion. A rectangular measuring diaphragm, which was narrow in the apical-basal dimension (2 μm) for greater resolution in detecting a gradient of grains, was used. It was wide in the lateral dimension (usually 20 μm) for greater sensitivity, though still small enough to pass between nuclei. A rotating stage permitted alignment of the diaphragm with the cell-chorion border and allowed for movement along the basal-apical axis by means of a single stage control. To this stage control, a spring-loaded fine micrometer head was attached which facilitated measurements at predetermined distances. Positioning of the diaphragm, initially adjacent to the cell-chorion border, was achieved by visualizing simultaneously the images of the cell and the silver grains within the measuring area (Fig. 3*c*). For each measurement, the transmitted light was interrupted, the image of the silver grains alone (Fig. 3*d*) was diverted to the photometer, the reflected light intensity was recorded electronically, and the stage control was advanced in preparation for the next measurement.

Regions of the follicular epithelium exhibit differences in the pattern of secretion (Fig. 4) corresponding to localized differences in the chorion structures produced (18). For this reason, all measurements were made in the predominant region of the follicle known as "flat" (Fig. 1), in which the cells are characterized by similar secretion behavior. In most experiments, 30 cells widely scattered in the flat region in two different sections were analyzed at 10-μm intervals. In some experiments, five closely grouped cells in a single section were analyzed at 2- or 3-μm intervals to define in greater detail the grain distribution near the apical border.

Computer Analysis of Photometric Data

A computer program was developed to analyze the photometric measurements. In this program, a background due to reflectance of the section itself, background grains, and light intrinsic to the microscope is substracted from each measurement. To make the graphs from different experiments directly comparable, normalization is then performed for both the spatial dimension and the grain density. Spatial normalization is

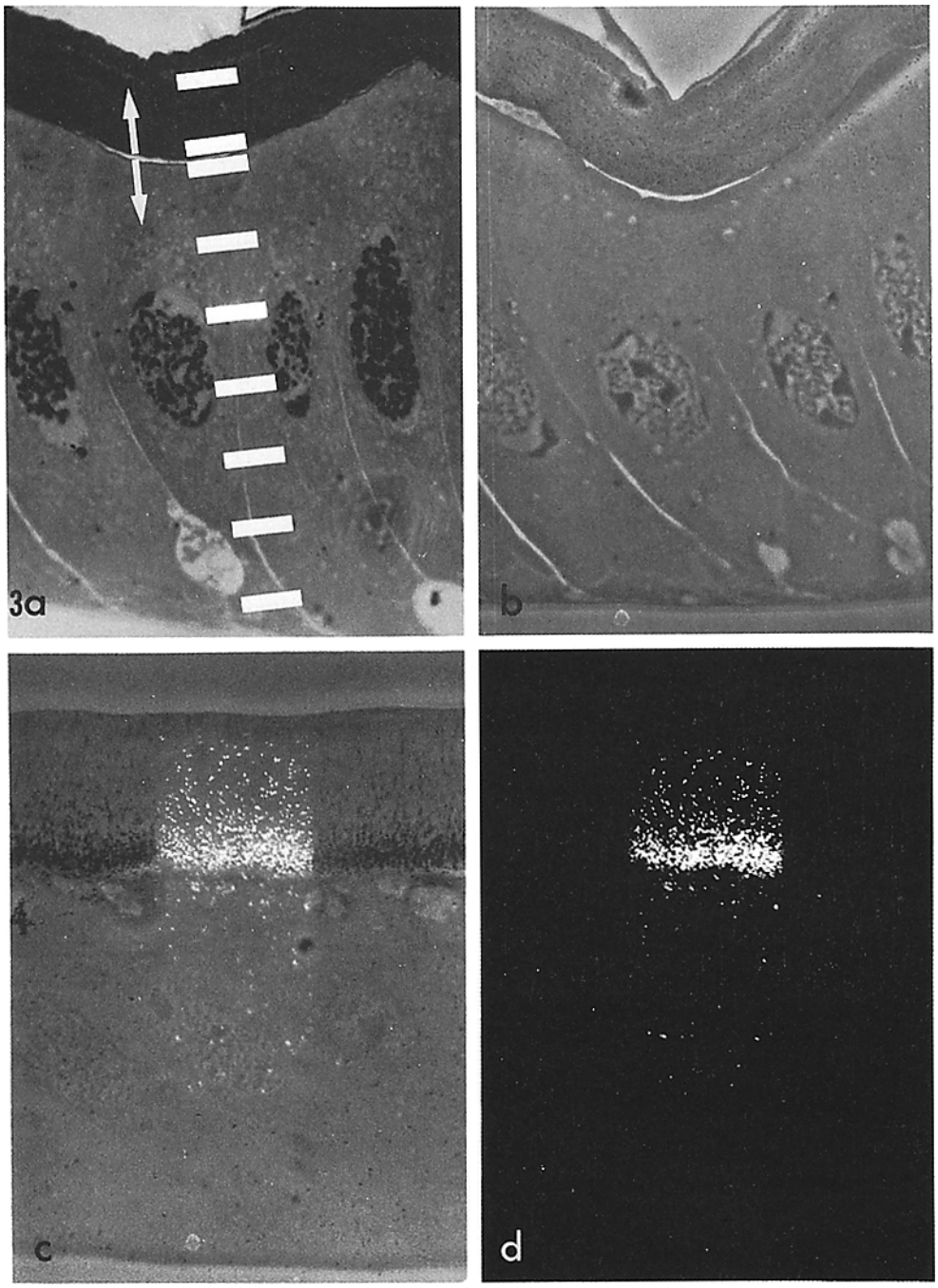

FIGURE 3 Method for selecting the fields and taking photometric measurements. × 1,100. (*a*) Toluidine blue-stained section of the follicular epithelium. Note the elongate and centrally located nuclei and the darkly stained chorion at the top. The relatively unstained cytoplasmic areas correspond to Golgi zones interspersed among the basophilic rough endoplasmic reticulum (data not shown). The white rectangles diagram the progression of measurements across the cell and chorion. The measuring diaphragm is first positioned adjacent to the cell-chorion border and then advanced in equidistant steps across the cell, in a path avoiding the nuclei, until the basal end is reached. The diaphragm is then returned to the cell-chorion border and a similar progression in the opposite direction across the chorion is made. (*b*) An unstained section, showing that the relevant features (position of nuclei, cell-chorion border, surfaces of cell and chorion) are easily visible using phase contrast. (*c*) A section examined by phase contrast using transmitted light, with a simultaneously vertically illuminated area (large upright rectangle). (*d*) The same field as in Fig. 3*c*, after the transmitted light was blocked, as during photometry. Only the vertically illuminated silver grains are visible.

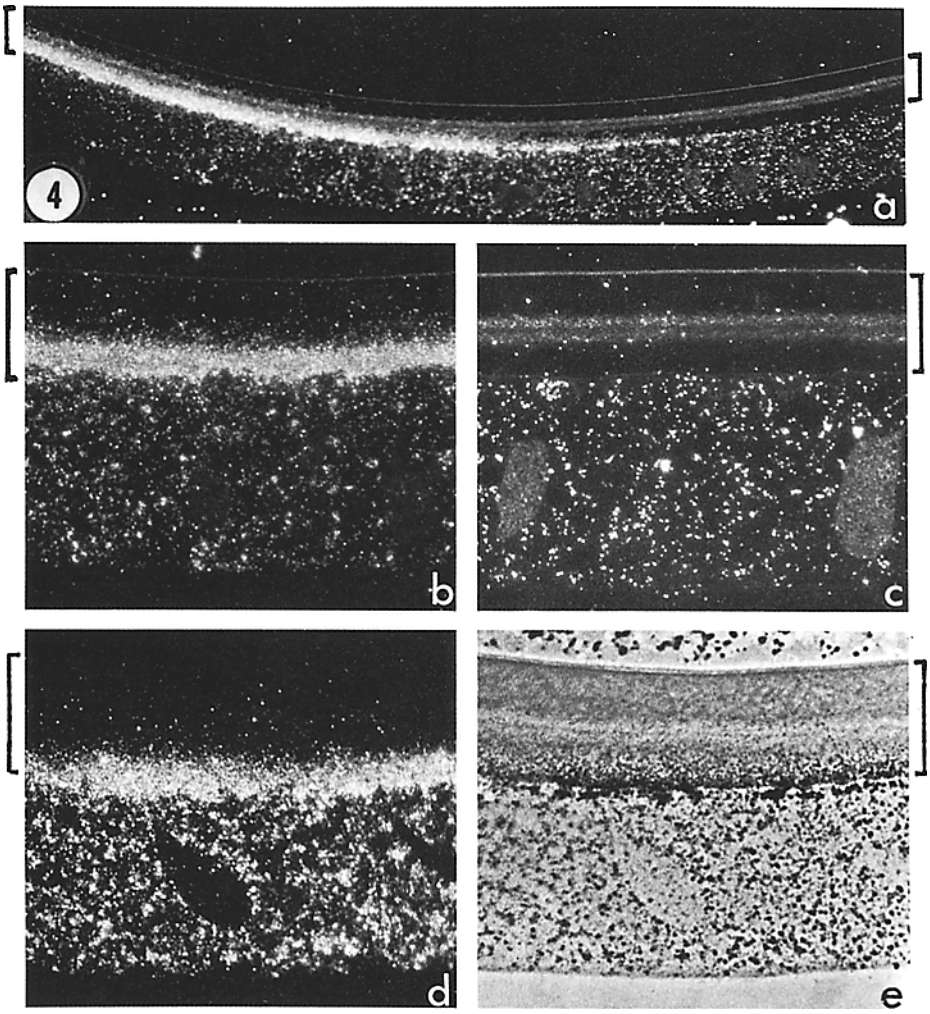

FIGURE 4 (*a–c*) Regional variation in secretory kinetics of the follicular epithelium. Dark-field illumination, fractional position 0.24, 2.5-min pulse, 15-min chase. The low power autoradiogram (Fig. 4*a*, × 150) shows the flat region of the epithelium at right and the zone of aeropyle crowns (i.e., specialized air channels [26]) at left. The two zones are shown in Fig. 4*c* and *b*, respectively, at higher magnification (× 410). Note the differences in silver grain distribution. (*d* and *e*) Photographs of the same section, showing that even when much of the secretion is in the border area, the cell-chorion border is identified easily by phase microscopy (Fig. 4*e*), although not in dark field (Fig. 4*d*). Stage VIII, 6-min pulse, 10-min chase, × 410. In this and subsequent figures, the chorion is indicated by black brackets.

necessary for each cell because of differences in orientation. Normalization of the grain density is necessary because of random differences in incorporation by different follicles or cells; the differences are inconsequential, since for any cell both cytoplasm and chorion (secreted and nonsecreted proteins) are analyzed.

For plotting the data points along the abscissa (spatial dimension), the cell-chorion border is assigned spatial position zero, and distances from it are given negative and positive values for cell and chorion, respectively (Fig. 5). The computer program takes into account prespecified average thicknesses for cell and chorion, distance between adjacent measurements, and the number of measurements actually made in a particular progression through cell or chorion. Thus, for example, if the "real" cell thickness is 55 μm, all measurements from a single progression at 10 μm are positioned in the graph between −55 and 0 μm (Fig. 5, left), using the appropriate scaling factor, whether the measurements are six (radial orientation) or more (oblique cell orientation or measuring path). No vertical adjustment is performed at this point. The data from additional progressions are

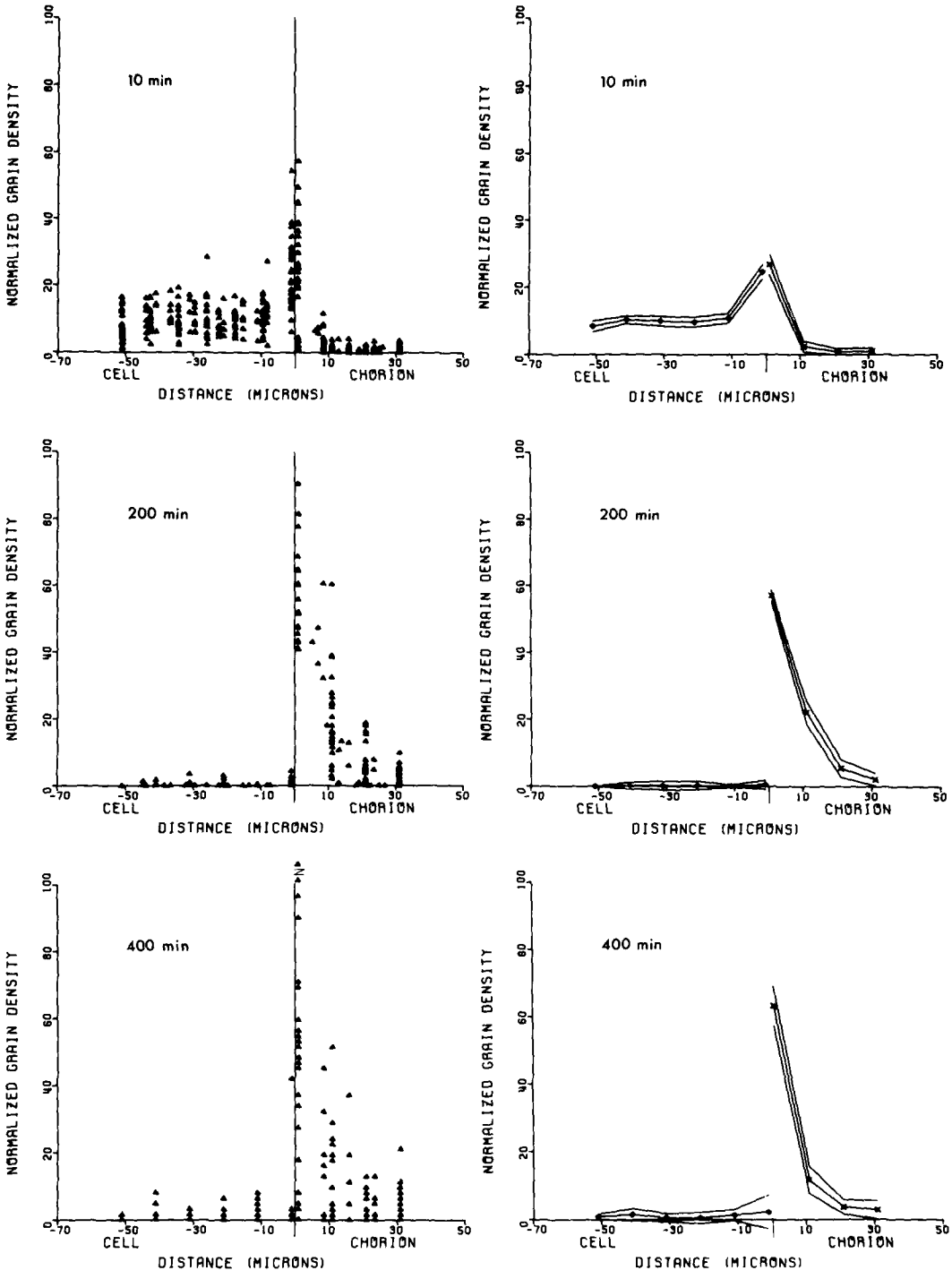

FIGURE 5 Quantitative analysis and plotting of autoradiographic data by computer. Follicles of stages VII–VIII were labeled for 6 min with [^{3}H]glycine and chased for 10, 200, and 400 min. Photometric data were obtained as diagrammed in Fig. 3*a*, at 10-μm intervals. The left panels show the background-corrected data as positioned by the computer relative to the real dimensions of cell (−55 to 0 μm) and chorion (0 to 35 μm). The vertical line indicates the cell-chorion border. In the right panels, the mean measurements are plotted with their standard errors. For further details, see the text.

similarly processed and pooled into an appropriate number of spatial "bins" (six cellular bins in the above example: one for the border and one for each adjacent "real" 10-μm distance toward the basal end). The mean grain density in each bin is then determined.

The scaling factor for the ordinate, S_o, is calculated by setting

$$S_o = K \frac{N}{\Sigma \bar{d}},$$

where K is a constant, N the number of bins in cell plus chorion, and $\bar{d}$ the mean density for each bin. This operation has the effect of approximately equalizing for different experiments the area under the curve of normalized grain density vs. normalized distance (i.e., approximating the condition of equal numbers of grains per cell plus chorion; the approximation improves as the number of bins increases).

The computer finally directs the plotting of all data for a particular tissue sample, using the appropriate scaling factors. The program is very versatile. It can plot the data individually (Fig. 5, left), in terms of bin means, or in terms of bin means with standard error of the mean indicated (Fig. 5, right). It can add separately all the values for cell and for chorion, thus determining the percentage of the total radioactivity which is found in the intracellular chorion at each chase time. It can plot the data from several experiments together (Fig. 6). This computer analysis of photometric data is described in detail elsewhere.[1]

Electron Microscope Autoradiography

For electron microscope autoradiography, silver sections were collected on 300-mesh copper grids coated with Formvar and carbon. Sections were covered with Ilford L4 nuclear track emulsion, using the loop method of Caro and van Tubergen (6). Autoradiograms were exposed in light-tight boxes containing desiccant at 4°C for 7 mo. After processing with Kodak Microdol-X developer for 5 min at 20°C, emulsion gelatin was removed by immersion of grids for a total of 30 min in three changes of 0.1 N NaOH. Sections were stained in 1% uranyl acetate for 10 min and in Reynolds (29) lead citrate for 4 min and examined with a Philips 300 microscope.

Dissection of Chorion and Epithelial Fractions

Cut and washed follicles were frozen and then thawed directly in either 1% H_2O_2 or 95% ethanol, adjusted to 0.05 M sodium acetate, pH 5, at 0°C. The chorion and epithelium were separated from each other by dissection, using watchmaker's forceps and siliconized pipettes. Scanning electron microscopy showed no cytoplasmic debris associated with the chorion after dissection. The epithelium or its fragments plus the dissection medium were precipitated with TCA. The resulting pellet (epithelium and any extracted proteins) and the chorion were each solubilized by adding equal volumes of electrophoresis sample buffer (1% 2-mercaptoethanol, 1% SDS, 6 M urea, and 10 mM Tris-HCl, pH 8.4 [25]) and incubating at 90°C for a maximum of 1 h. For measurements of total radioactivity, aliquots were precipitated with 20% TCA, filtered on glass fiber filters, and counted by liquid scintillation.

SDS-Polyacrylamide Gel Electrophoresis

Samples solubilized in electrophoresis sample buffer (described above) were carboxamidomethylated with iodoacetamide and analyzed by electrophoresis on highly cross-linked gels; the gels were stained, and the profiles of bulk and newly synthesized proteins were determined by measurements of optical density and radioactivity, respectively, as previously described (25, 26). Data were analyzed by computer (40).

RESULTS

Autoradiographic Kinetics of Intracellular Protein Transport and Discharge

The kinetics of intracellular protein transport and secretion were examined by autoradiography in 153 follicles, combining a number of different animals and developmental stages. The follicles were labeled for brief periods with tritiated amino acids (1–6 min), chased for variable periods of time, fixed, processed for autoradiography, and used for quantitative analysis of the spatial distribution of radioactivity.

The secretion kinetics obtained were consistent among experiments; one example is presented in Fig. 6. Initially, the labeled proteins were present throughout the cytoplasm (for the first 18 min following the end of the pulse, in this case). Label began to accumulate in the apical cell region and to be discharged into the chorion between 18 and 22 min. This process continued until 32 min, when discharge was essentially complete. In the interval from 18 to 32 min during which secretion occurred, the grain density in much of the cell declined uniformly without distinguishable basal to apical differences. However, the grain density in the extreme apical region first rapidly increased and then gradually declined. This pattern of translocation of labeled protein is especially evident in Fig. 7 in which the density in cellular regions

[1] Blau, H. M., C. Lu, and F. C. Kafatos. Manuscript in preparation.

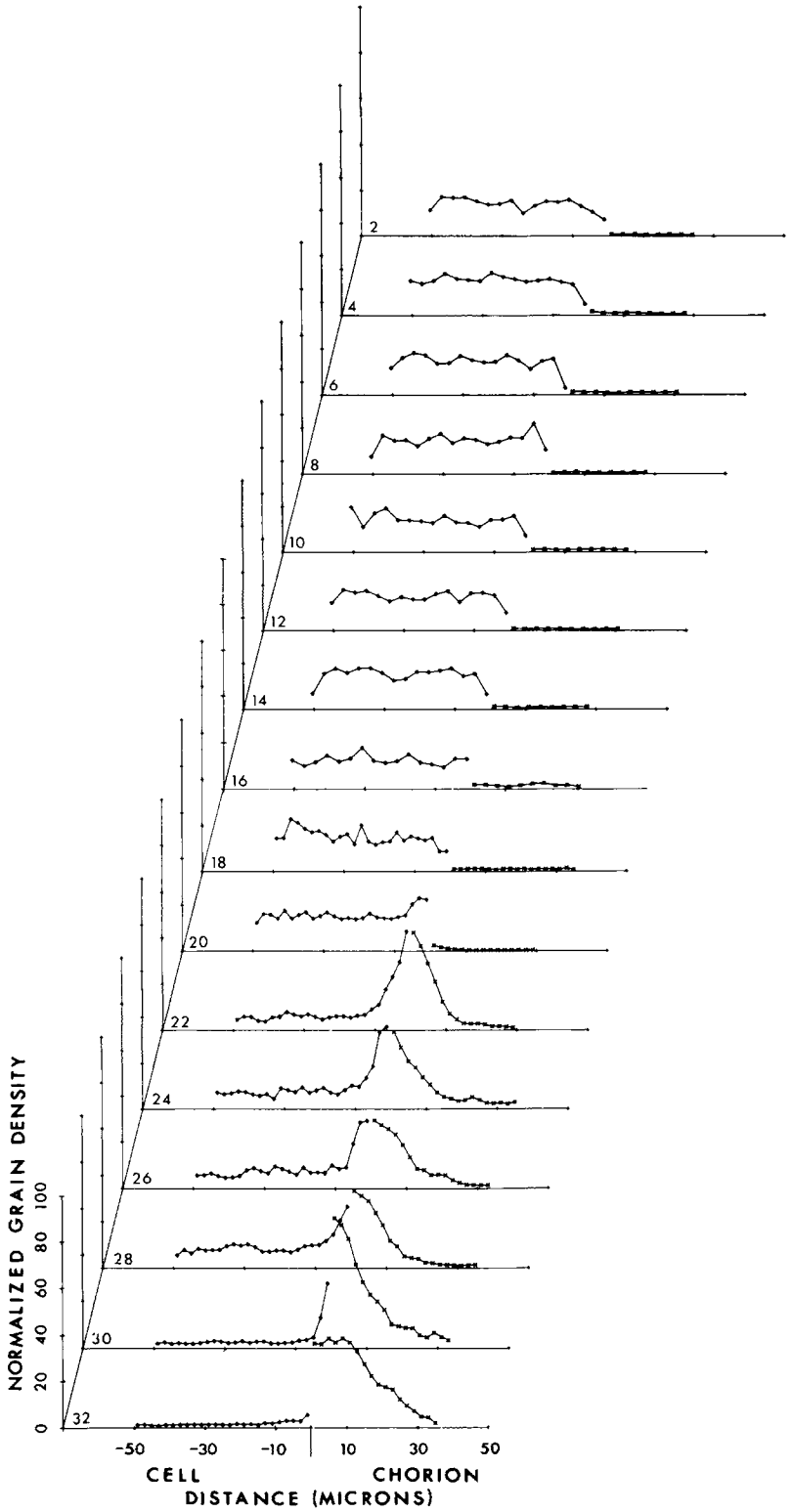

FIGURE 6 Detailed kinetics of intracellular transport and discharge. Follicles of fractional positions 0.41–0.47 were labeled for 2 min with [^{3}H]glycine, chased for 2–32 min, and processed for autoradiography. Measurements were taken at 3- or 2-μm intervals (before or after 16 min of chase, respectively). Note the uniform labeling of all subapical cell regions and their even draining during secretion. Note also the transient accumulation of label in the apical region between 20 and 32 min. By contrast, the gradient of grains within the chorion is not transient, but a stage-specific property (see also Figs. 10 and 11).

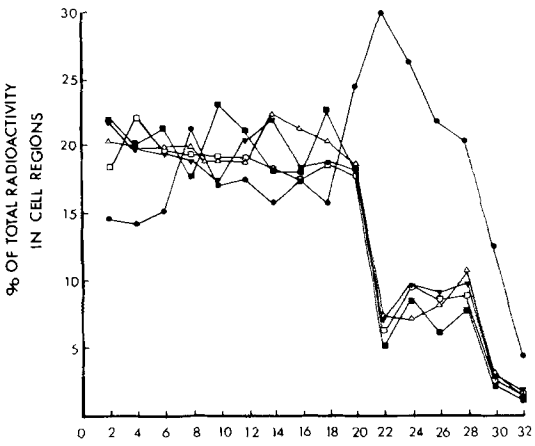

FIGURE 7 The kinetics of removal of label from the apical region of follicular cells (●) and from regions located progressively farther, as far as the basal surface (△, ▲, □, ■, respectively). Cells were divided into five equal regions, and grain densities in each region were plotted relative to the total for cell plus chorion. Note the initially constant density in the subapical regions and their subsequent uniform drainage. Note also the pronounced accumulation of label in the apical region between 18 and 22 min, and the subsequent slower loss of label from this compartment. The data are from the experiment shown in Fig. 6.

along the basal-apical axis was plotted as a function of chase time.

These results show that the labeled protein resides in all regions of the cytoplasm for many minutes before beginning to accumulate near the apical border in preparation for discharge from the cell. In contrast to this time-consuming residence throughout the cytoplasm, the movement of labeled proteins to the apical border seems rapid. This is evident since at all times the subapical regions are almost indistinguishable in terms of grain density, and show no gradients, i.e., the basal cytoplasm is not drained of labeled protein before the middle of the cell. Similarly, the discharged proteins quickly reach their ultimate distribution within the extracellular chorion (Fig. 6).

An analysis of the results of all experiments reveals that accumulation of the radioactivity in the apical region and discharge begin between 10 and 20 min, and discharge is essentially complete between 30 and 60 min. It is noteworthy that no difference was evident when the areas immediately above and below the nuclei were compared to the areas lateral to them, which were normally sampled.

Pathway for Intracellular Transport of Labeled Protein before Discharge

The quantitative results presented thus far are supported qualitatively by the representative dark-field autoradiograms from two separate series of experiments shown in Fig. 8. This figure also documents a microheterogeneity of grain distribution which is too fine to be registered by our photometric methods. Immediately after a 1-min pulse, label is distributed relatively uniformly throughout the cytoplasm. After 1–2 min of chase, the label shows some evidence of clumping, and by 4 min of chase the clumping is pronounced. The clumped pattern persists until most labeled chorion proteins have been discharged; the nonsecreted proteins are predominantly distributed in a nonclumped pattern (Fig. 8, left, 30 min).

To resolve the structure associated with the clumped pattern of grains, preliminary EM autoradiography was performed on silver sections cut from selected blocks previously examined by light microscope autoradiography. The follicles had been labeled for 1 min with [^{3}H]glycine and subsequently chased for 0 or 8 min before fixation. Due to our limited objective, no quantitative analysis was performed; approximately 15 sections and 25 micrographs were examined for each time point. Typical results are shown in Fig. 9.

After 0 min of chase, the label was localized predominantly over the rough endoplasmic reticulum (rER) which occupies much of the cell volume; association with Golgi elements was less frequent. By 8 min, the label was almost entirely associated with the Golgi elements, which are distributed throughout the cytoplasm much like the grain clumps noted by light microscopy (Fig. 8; see also Fig. 3*a*). It appears that the secretory proteins are associated with the Golgi apparatus during the time-consuming step before movement toward the apical region. Definitive conclusions about the intracellular compartments through which the proteins pass await future cell fractionation and quantitative electron microscope autoradiography.

Labeled Protein Distribution within the Chorion at Different Developmental Stages

Figs. 6 and 8 reveal a graded distribution of labeled protein within the extracellular chorion, with the greatest density nearest the secretory cell.

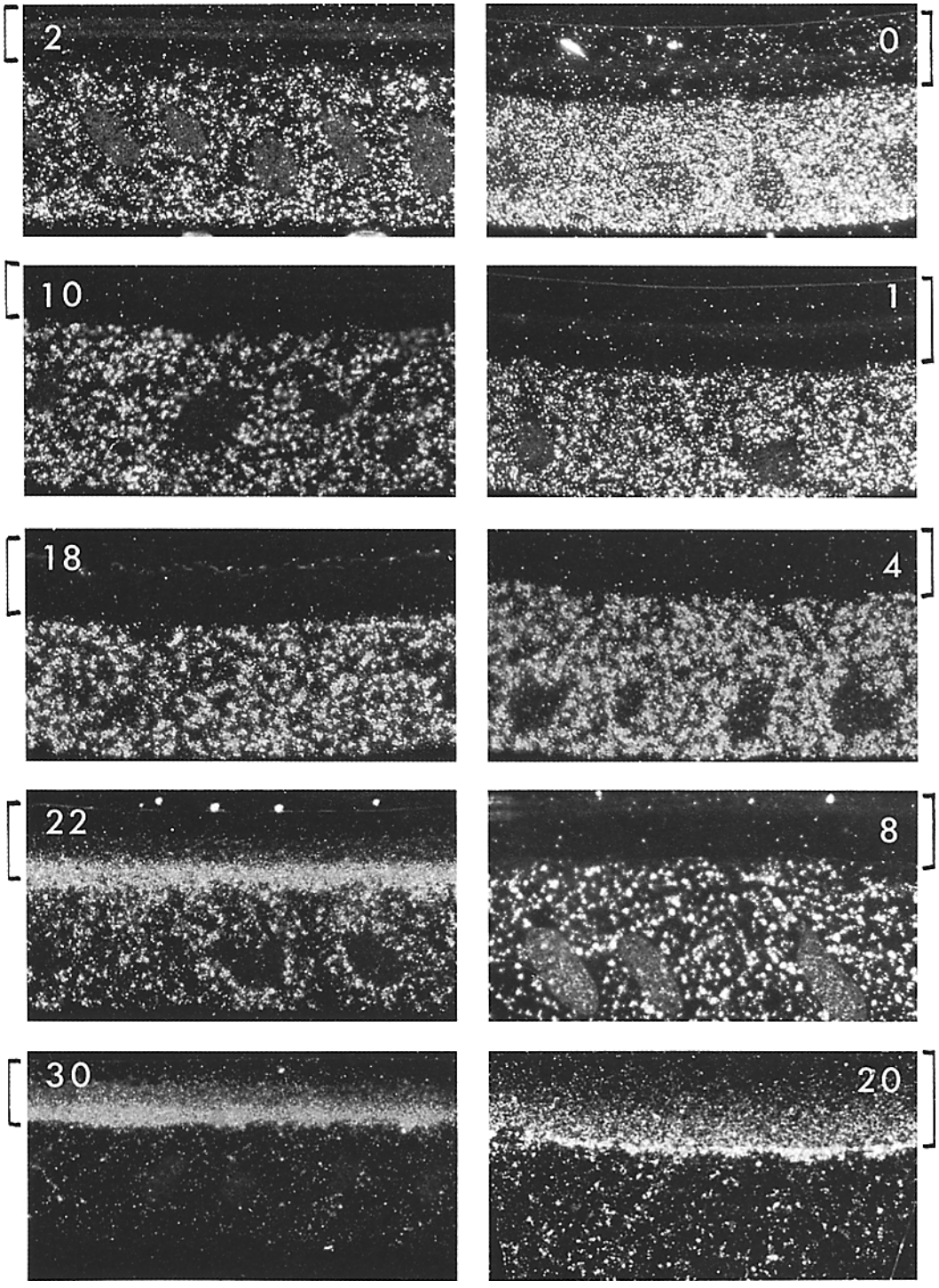

FIGURE 8 Clumping of radioactivity in the follicular cells, developing shortly after the end of the pulse and persisting until secretion is completed. Representative autoradiograms from two experiments are shown; dark-field illumination, × 370. The experiment shown on the left was the same as in Figs. 6 and 7. The experiment on the right used a 1-min pulse of [^{3}H]glycine and follicles of fractional positions 0.37–0.44. The chase durations, in minutes, are indicated with each autoradiogram.

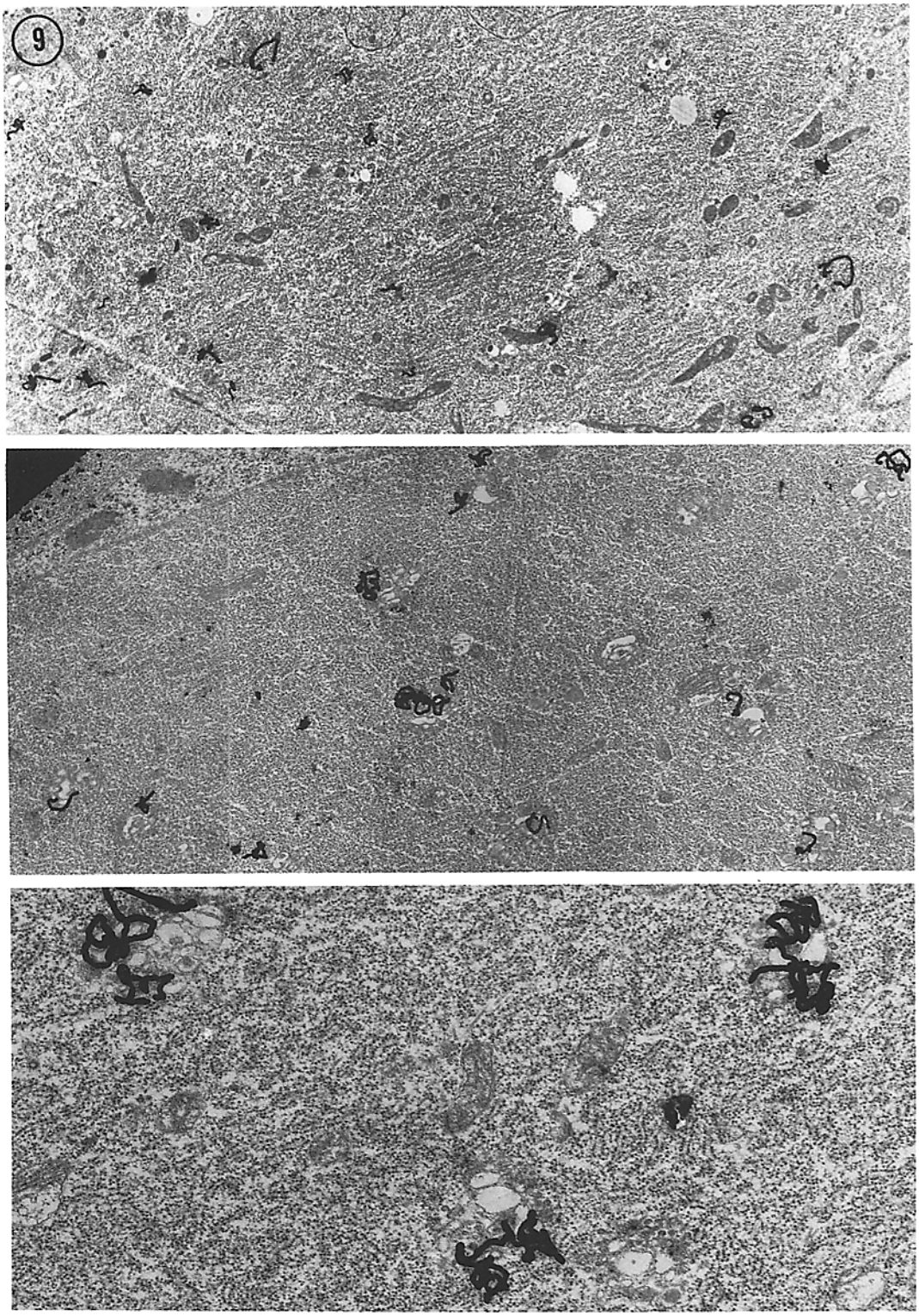

FIGURE 9 Identification of organelles involved in secretion. Selected follicles from the experiment of Fig. 8, right, were analyzed by electron microscope autoradiography. After a 1-min pulse and no chase (*top*), grains were localized primarily over areas of rough endoplasmic reticulum throughout the cell, and more rarely near Golgi elements. After 8 min of chase (*middle* and *bottom*), grains were almost invariably Golgi-associated. × 6,800 for top and middle, × 19,300 for bottom.

This gradient does not change substantially with time after discharge (Fig. 10) and, thus, is not a transient result of slow diffusion but rather a stage-specific developmental property (Fig. 11). The first quarter of choriogenesis was not investigated. Fig. 10 shows that, in the second quarter (stages III-V), labeled protein is distributed nearly uniformly throughout the chorion. In the third quarter (approximately stages VII and VIII), a clear gradient is evident, and in the last quarter (stages VIII-Xc), the gradient is so steep that labeled protein is found almost exclusively in a narrow layer adjacent to the secretory cells. The relevance of this changing label distribution to the complex morphogenesis of the chorion structure is discussed in detail elsewhere.[2]

Kinetics of Secretion Studied by Dissection of Chorion and Epithelium

Dissection of the chorion from the epithelium is convenient for determining the overall kinetics and essential if the discharged and nondischarged protein fractions are to be recovered and analyzed. Since the chorion proteins are only gradually cemented together with disulfide bonds (5, 18), newly secreted chorion proteins can be extracted with relative ease. Dissection of the epithelium from the chorion in the presence of H_2O_2 helps retain newly secreted proteins within the chorion.[2] Fig. 12 shows the overall kinetics of secretion as determined by dissection. Any proteins extracted by the dissection medium appear in the cellular fraction, because the medium is precipitated with TCA together with the epithelium (see Materials and Methods). 95% Ethanol is as effective as H_2O_2 in minimizing extraction, although it makes dissection somewhat more difficult.

Fig. 13 compares the kinetics determined by autoradiography (*A*) and dissection (*B*). The comparison was limited by the inclusion in the dissection experiment of cells from the nonflat regions known to have different secretion kinetics (see Fig. 4), as well as by the use of different labeled amino acids. In the chorion, the amino acid glycine is more abundant than leucine, and, since glycine was used for autoradiography and leucine for dissection, we would expect the final percentage of radioactivity in the chorion to be higher in the autoradiographic experiment. Within these limits, the results were in quite reasonable agreement. In this experiment, the time necessary for half of the labeled chorion proteins to be secreted (half-secretion time, t_{50} [17]), counted from the middle of the pulse, was estimated as 23–27 min by dissection, and 20–23 min by autoradiography. Discharge was essentially complete in 30–50 min. Fig. 13 also compares the kinetics for different developmental stages. The differences are minor, both in half-secretion time and in percent of radioactivity ultimately associated with the chorion.

Fig. 14 summarizes a more extensive series of experiments. For all stages combined, the half-secretion time (corrected for pulse duration) was 24.5 min (range: 16–33 min) in the dissection experiments, and 20.5 min (range: 18–23 min) in the autoradiography experiments. The maximum radioactivity associated with the chorion was 85.5% of the total (range: 75–96%, leucine) and 96.5% (range: 94–99%, glycine), respectively.

Secretory Kinetics of Different Chorion Proteins

A double-label experiment was designed to examine whether all chorion proteins synthesized at a particular stage are discharged in parallel. Follicles in mid-choriogenesis (fractional position 0.5, stages V–VI) were labeled for 30 min with [^{14}C]leucine and then chased for 45 min to permit discharge of essentially all labeled chorion proteins. The follicles were then labeled for 3 min with [^{3}H]leucine and chased for 10, 20, 30, 40, or 50 min. Finally, the cellular and the chorion fractions were separated by dissection and their proteins were dissolved and analyzed by electrophoresis followed by slicing the gel and counting the radioactivity by liquid scintillation.

Fig. 15 shows typical results for the chorion fraction. In this experiment, the fully discharged ^{14}C-proteins served as an internal standard, against which the partially or fully discharged ^{3}H-proteins were compared at various times of secretion. As expected, when the ^{3}H-proteins had been almost fully discharged (50 min, 86% in the chorion), their profile was nearly indistinguishable from that of the fully discharged ^{14}C-standard. The noteworthy observation was that at early (10 min) and middle (20 min) secretion times, the profile of partially discharged (9 or 51%, respectively) ^{3}H-proteins was also identical.

Fig. 15, right, compares the ^{3}H and ^{14}C profiles

[2] Blau, H. M., and F. C. Kafatos. Manuscript in preparation.

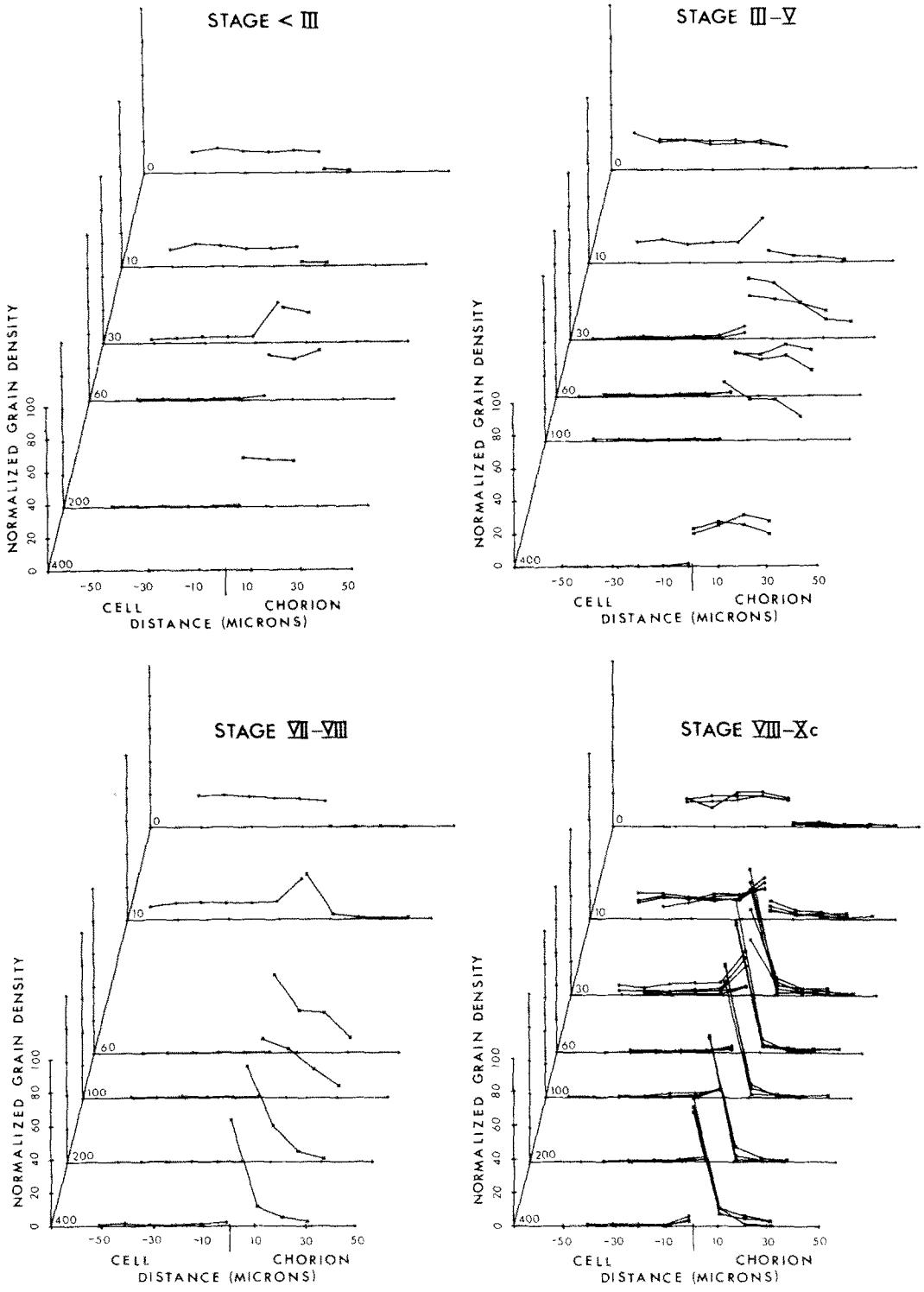

FIGURE 10 The kinetics of secretion and the extracellular distribution of label at different developmental stages. Follicles were labeled for 6 min with [^{3}H]glycine and chased for the indicated period (logarithmic scale). The follicles before stage III were not staged according to protein synthesis because of their fragility, and are indicated as <III. Plots were grouped together by stage, to show complete permeation (<III), complete to graded permeation (III-V), graded permeation (VII-VIII), and surface apposition (VIII-Xc).

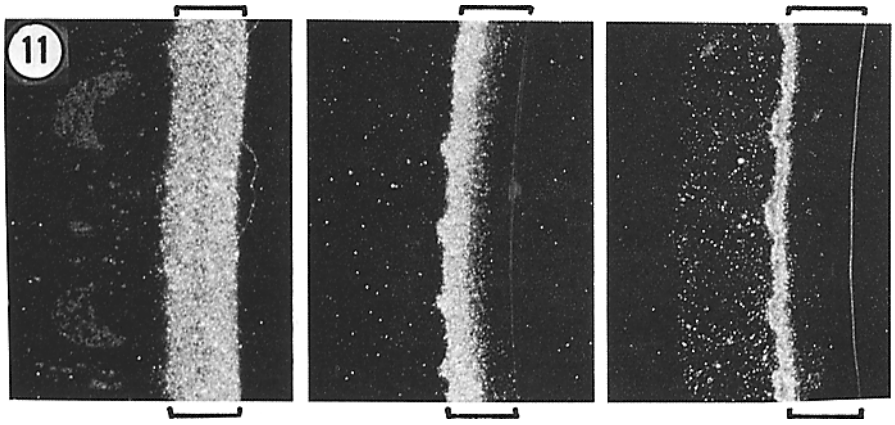

FIGURE 11 Different distribution of labeled proteins within the chorion at different developmental stages. Glycine-labeled autoradiograms are shown after attainment of the definitive grain distribution: complete permeation of the chorion (stage III, *left*), graded permeation (stage VII–VIII, *middle*), and surface apposition (stage X, *right*). In each panel, the cell is at the left and the chorion is indicated by horizontal brackets. × 285.

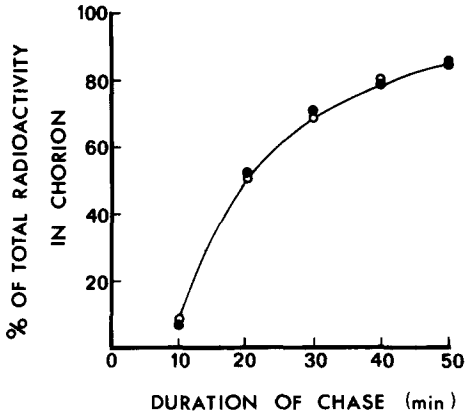

FIGURE 12 Overall kinetics of secretion determined by dissection of epithelium from chorion in 1% H_2O_2 (●) or 95% ethanol (○). Follicles of fractional position 0.5 were labeled with [^{3}H]leucine for 3 min, chased as indicated, cut in half, and washed free of yolk. One-half of each follicle was dissected in each of the two media. The epithelial and the chorion fractions were separately analyzed for TCA-precipitable radioactivity. The plot shows the radioactivity in the chorion relative to that in chorion plus epithelium.

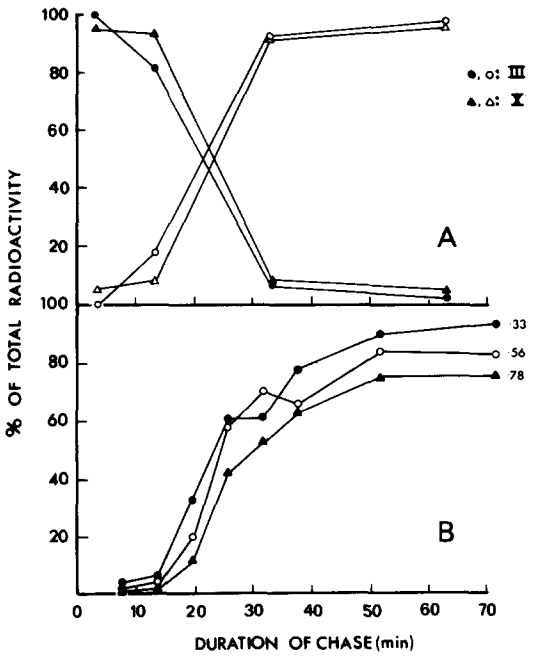

FIGURE 13 Overall kinetics of secretion determined autoradiographically (*A*) or by dissection in H_2O_2 (*B*). The top panel shows the proportion of total radioactivity in cell (●, ▲) and chorion (○, △ at two stages, from the experiment of Fig. 10); the crossover point at 50% is the half-secretion time. The bottom panel shows the progressive accumulation of radioactivity in dissectable chorion, at three developmental stages labeled with [^{3}H]leucine for 3–4 min (fractional positions 0.33, 0.56, and 0.78). All chase durations were calculated from the middle of the corresponding labeling period.

in greater detail, showing the isotope ratio at each gel slice, together with the 95% confidence limit for counting (40). In regions of significant radioactivity, the ratio showed only minor deviations from constancy. These deviations were consistent in all samples, and thus could not be due to asynchronous discharge. In fact, the deviations were expected from the known developmental

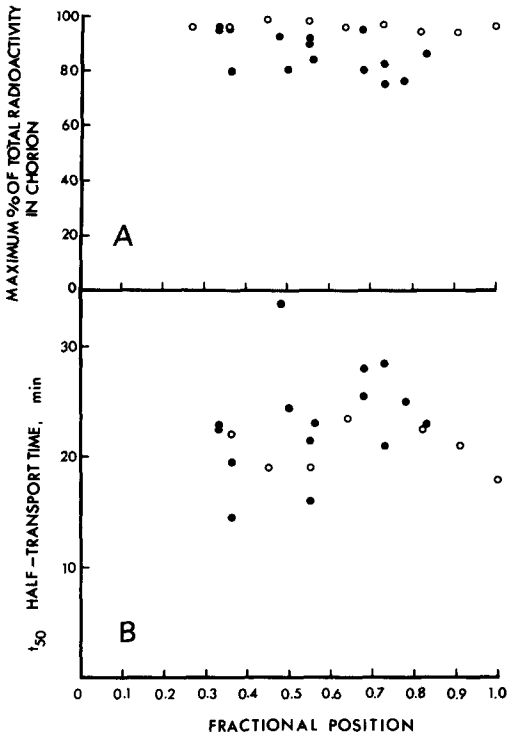

FIGURE 14 Transport kinetics at different developmental stages. The maximum proportion of total radioactivity which was associated with the extracellular chorion is shown in (*A*), and the half-secretion time is shown in (*B*). The data were obtained by autoradiography (○) from an experiment using a 6-min pulse of [^{3}H]glycine, and by dissection (●) from experiments using a 3- or 4-min pulse of [^{3}H]leucine and dissection in 1% H_2O_2. All chase durations were calculated from the middle of the corresponding labeling period.

changes in synthetic profile during organ culture (26). During the 1 h intervening between the midpoints of the two labeling periods, the relative synthetic rates of components B_2 and $A_{3,4}$ (indicated by dots in Fig. 15, right) decreased, as they should, resulting in a lowered ratio.

We conclude that, within the electrophoretic resolution, all chorion protein subclasses synthesized at mid-choriogenesis are discharged at the same time and do not exhibit differential secretory kinetics.

DISCUSSION

Quantitative Autoradiography

The quantitative autoradiographic methods used in this study are simple and convenient, once adjusted to the requirements of a particular cell type and standardized. They should have widespread application, not only for studies of secretion but also for quantitative documentation of spatial distributions of labeled molecules (e.g., in extracellular morphogenesis). Relative measurements will be generally preferable, in order to reduce variability. In the present study, this was accomplished by sampling all relevant compartments within each cell and by normalization. For determination of absolute grain density, it is possible to include in each block a sample of polymerized labeled Araldite ([8] see also Fig. 1); this serves as an internal standard, permitting correction of the photometric signal for random variations, e.g., thickness of section or emulsion and conditions of exposure or development.

The Secretory Pathway

A secretory pathway involving sequentially the rER, the Golgi apparatus, and secretory granules operates in many cell types (16). This also appears to be the pathway used for chorion protein secretion. Strong evidence is derived from a group of osmiophilic, high cysteine chorion proteins which are localized in Golgi elements and in small dense secretory granules in the follicles of the silkmoth *Bombyx mori*.[3] This conclusion is also supported by our results which show that, shortly after synthesis, labeled chorion proteins become associated primarily with Golgi elements. This association is indicated by preliminary electron microscope autoradiography (Fig. 9), as well as by the clumped distribution of grains throughout the cytoplasm in light microscope autoradiographs (Fig. 8), in a pattern corresponding to the distribution of Golgi elements (data not shown; see also Fig. 3*a*). Similar clumped patterns, immediately after a pulse of [^{3}H]galactose in thyroid tissue, were interpreted by Whur et al. (39) as indicative of localization in the Golgi apparatus. To define unequivocally the organelles of the secretory pathway in follicular cells, quantitative analysis of electron microscope autoradiograms and cell fractionation studies will be necessary.

Overall Secretory Kinetics

Secretory kinetics are known to vary widely in different types of cells, even within the same animal. In the silkmoths, we have shown that the half-secretion time is 20–25 min for the follicle,

[3] Mazur, G. D., and F. C. Kafatos. Unpublished observations. See also Figs. 13 and 18 in reference 18.

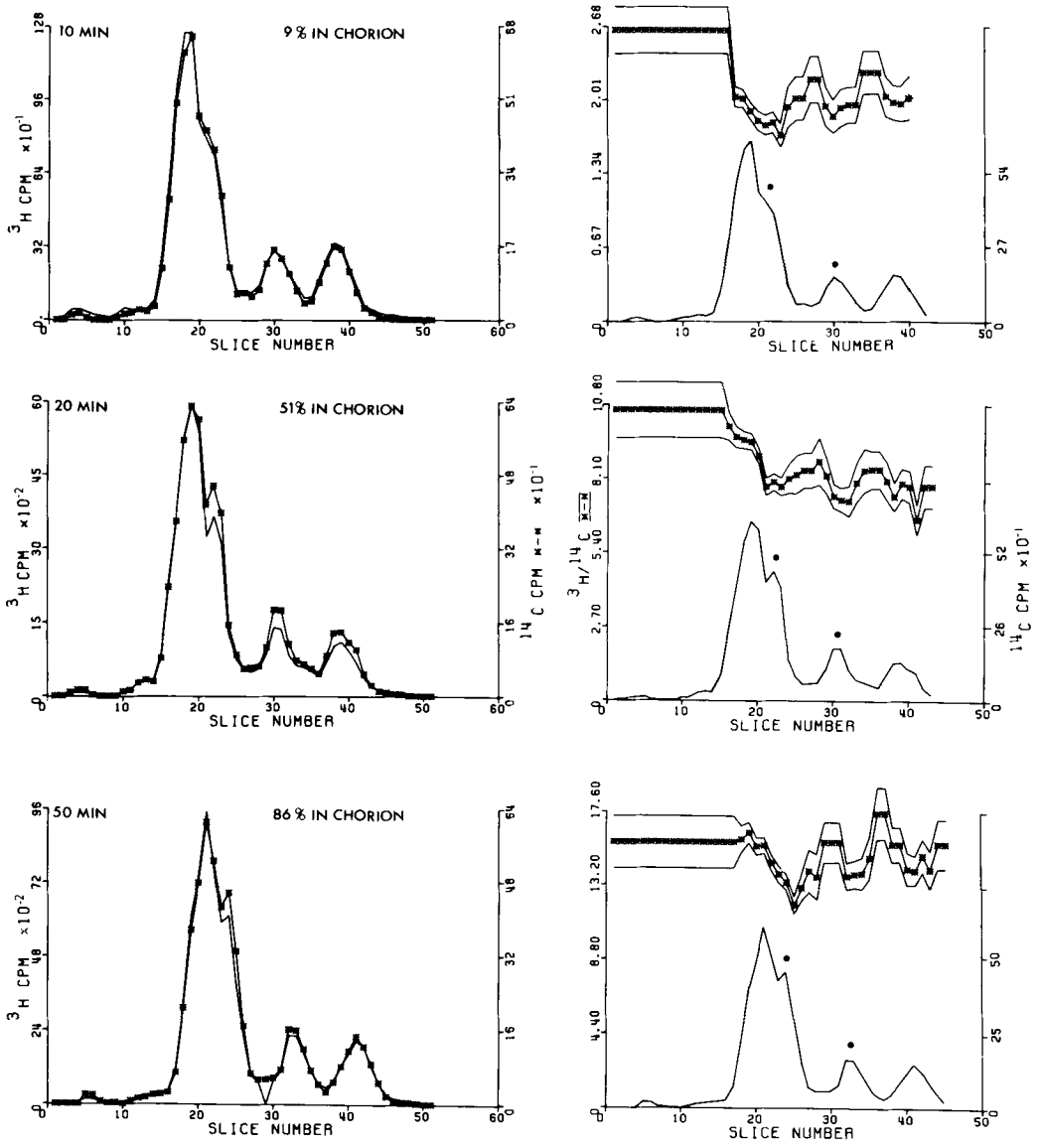

FIGURE 15 Parallel discharge of different chorion proteins. Follicles of fractional position 0.5 were pulse-labeled with [^{14}C]leucine (280 mCi/mM, 9.4 μCi/ml) for 30 min and then incubated for 45 min in chase medium. Subsequently, a 3-min pulse of L-[4,5-^{3}H]leucine (33.6 Ci/mmol, 2 mCi/ml) was administered and the follicles were chased for 10, 20, 30, 40, and 50 min. After the follicles were cut in half and washed, they were dissected in 95% ethanol and the epithelium and chorion fractions were dissolved and assayed separately for total TCA-precipitable radioactivity. The ^{3}H radioactivity in the chorion expressed as percentage of that in epithelium plus chorion is indicated at the top of each left panel, together with the duration of chase. Aliquots of each sample were analyzed by SDS-polyacrylamide gel electrophoresis. The left-hand panels show ^{3}H (−) and ^{14}C (*) electrophoretic profiles of the chorion fraction at selected chase times; the right-hand panels show the same ^{14}C profiles (−), together with the corresponding ^{3}H/^{14}C ratio and the associated confidence limits for counting error (±). The partially (10 min) to fully (50 min) discharged ^{3}H-chorion proteins show identical profiles, when related to the internal ^{14}C standard. The deviations from ratio constancy are similar at all chase times, and correspond to the expected change in the profile of proteins synthesized (decrease in proteins B_2 and $A_{3,4}$, left and right dots, respectively) in the interval between the ^{14}C and ^{3}H pulses. For further details, see the text.

compared with 74 min for the galea at the peak of zymogen secretion (17) and 3.4 h for the colleterial gland (10).

Speed of secretion does not appear to depend on polarization of the secretory organelles. Thus, in the highly polarized acinar cells of the guinea pig pancreas and rabbit parotid cells, the half-secretion time is approximately 1 and 2 h, respectively, both in the resting state (transport to storage granules) and after secretogogue stimulation (7, 15, 16). By contrast, the half-secretion time does not exceed 0.5 h in the follicular cells and in the resilin-secreting epithelial cells of the desert locust (38), both of which have Golgi complexes and rER distributed throughout the cytoplasm.

Polarization of organelles is also not dictated phylogenetically, since vertebrates have both polarized and nonpolarized cell types (23, 24, 28, 33, 37). It seems paradoxical that the insect tissues mentioned show a highly polarized direction of secretion though their rER and Golgi complexes are dispersed. It is possible that these cells secrete with a different polarity at earlier developmental stages (e.g., in forming the basement membrane, or in contributing the yolk-binding follicular protein [1]).

Little information is available concerning changes in secretory kinetics during differentiation (17). In the present study, no major changes in kinetics were detected in the last two-thirds of choriogenesis, when the profile of proteins being synthesized is continuously changing (26), as is their extracellular destination within the chorion. Preliminary results suggest that secretion is slower at some earlier stages, before peak secretory activity has been attained (5).

The Kinetics of Intracellular Transport

Although the intracellular transport pathway for secretory proteins has been traced in many systems, less is known about the time an average protein molecule spends in individual compartments of the pathway, and about the rate of movement between compartments. In studying the pancreas by EM autoradiography, Jamieson and Palade (14) showed that the peak of incorporated radioactivity is found in the rER immediately after the pulse, in the Golgi periphery 7 min later, in condensing vacuoles at 37 min, and in zymogen granules at 57 and 117 min. The kinetics of intracellular transport were similarly determined by Revel and Hay (28) for chondrocytes, Uhr (37) for myeloma cells, and Castle et al. (7) for parotid cells. Approximate kinetics can also be inferred from a number of other studies using EM autoradiography or subcellular fractionation.

In the present detailed kinetic study, two time-consuming steps were identified during the secretion of chorion proteins. The first is represented by the prolonged persistence of the clumped radioactivity pattern, which develops throughout the cytoplasm soon after pulse-labeling with amino acids (Fig. 8). The second is represented by the accumulation of labeled proteins at the cell apex before their discharge. This accumulation is visible just as discharge into the chorion begins, between 10 and 20 min, and persists until its completion.

Judging from the rapid appearance of the clumped grain pattern, in the follicular cells as in the pancreas, the time a protein molecule spends within the rER is very short, probably 1–2 min. The first time-consuming step appears to be associated with the Golgi apparatus and may be related to a pretransport "packaging" requirement.

When discharge of the labeled proteins begins, the subapical regions of the cytoplasm are uniformly drained of radioactivity; apart from the cell apex, no gradient is evident. This can only be explained by one of three models. (*a*) Prolonged packaging in the Golgi apparatus occurs *in situ* and the mature secretory granules produced are then transported toward the apical region. Polarized transport from nonpolarized packaging sites inevitably generates a gradient of transported granules, increasing in the direction of movement. Since such a gradient was not observed, the transport step must be very fast relative to the packaging steps, probably requiring <2 min. Thus, at steady state, transport involves a low proportion of the protein, and the gradient is obscured by the high background due to evenly distributed packaging sites. (*b*) No polarized transport occurs, but the packaging sites move constantly in all directions, and the mature granules are trapped in the apical region when they happen to enter it. The random motion of the sites must be rapid to mask the inverse gradient (basal end high) inevitably generated by such a mechanism. (*c*) Both random motion of packaging sites and polarized transport of mature granules occur. It is theoretically possible for the two processes to be relatively slow and yet fail to produce a gradient, if their rates are properly

balanced, but the probability of this coincidence seems rather remote.

Most likely, the parallel depletion of all subapical regions indicates that transport across the cells, whether random or polarized, requires relatively little time, and that the time-consuming step before accumulation in the apical region corresponds to a Golgi-associated maturation process, analogous to that observed in the pancreas (13, 14). This process might represent purely physical concentration and packaging or some post-translational covalent modification prerequisite to packaging or secretion. Glycosylation, acetylation, sulfation, and limited proteolysis are examples of modifications to which many secretory proteins are subjected. An established post-translational modification of chorion proteins involves charge modification of approximately one-third of the proteins (27).

The morphology of the cell apex indicates that the proteins are released into the chorion by exocytosis (data not shown). The apical accumulation of label suggests that a second time-consuming step is interposed between arrival of the secretory granules in the apical region and exocytosis. The nature of this step is unknown. It should be noted that secretory granules accumulate more abundantly in the apical region than elsewhere in the cell (5).

The distribution of labeled proteins within the chorion varies with developmental stage. This phenomenon has interesting implications concerning morphogenesis of this complex structure;[2] a substantial proportion of the chorion proteins reach their final destination by permeating a previously constructed framework, and thus much of morphogenesis occurs at some distance from the secretory cells (5, 35).

The Secretory Kinetics of Different Proteins

Fig. 15 and the constancy of kinetics during development indicate that, at least for the stages investigated and within the resolution of the electrophoretic gels, all secretory proteins are discharged with similar kinetics, irrespective of their molecular weight, final destination, and the occurrence or absence of charge modification. Scheele and Palade (34) and Tartakoff et al. (36) have arrived at similar conclusions in their biochemical studies of the exocrine pancreas. Such simultaneity is to be expected in view of the immunohistochemical studies of Kraehenbuhl and Jamieson (21). In other systems, the existence of different secretory granules for different products within the same cell has been documented (2, 3, 4). In all such cases, however, the products were synthesized at different stages of cell maturation, and were thus temporally as well as physically separated. There is no evidence thus far for different secretory kinetics of proteins which are synthesized simultaneously.

We thank Dr. C. Lu who did the programming and helped develop the computer analysis, Dr. J. Combs for his generous loan of equipment and for discussion, Drs. A. M. Tartakoff, R. D. Palmiter, L. Cherbas, and D. Shotton for their valuable discussions, Dr. M. G. Farquhar for her assistance in electron microscope autoradiography and critical reading of the manuscript, Dr. H. K. MacWilliams for constructing the dipping machine, M. Koehler for her help with figures, and M. J. Randell and A. K. Schilling for their secretarial assistance.

Dr. Kafatos was supported by grants from the National Science Foundation (BMS 72-02336) and National Institutes of Health (5R01 HD 040701) and Dr. Blau by a U.S. Public Health Service Training Grant (5T01 GH 00036).

Received for publication 23 November 1976, and in revised form 3 March 1978.

REFERENCES

1. ANDERSON, L. M., and W. H. TELFER. 1969. A follicle cell contribution to the yolk spheres of moth oocytes. *Tissue Cell.* **1**:633–644.
2. BAINTON, D. F., and M. G. FARQUHAR. 1968. Differences in enzyme content of azurophil and specific granules of polymorphonuclear leukocytes. II. Cytochemistry and electron microscopy of bone marrow cells. *J. Cell Biol.* **39**:299–317.
3. BAINTON, D. F., and M. G. FARQUHAR. 1970. Segregation and packaging of granule enzymes in eosinophilic leukocytes. *J. Cell Biol.* **45**:54–73.
4. BEAMS, H. W., and R. G. KESSEL. 1968. The Golgi apparatus: structure and function. *Int. Rev. Cytol.* **23**:209–276.
5. BLAU, H. M. 1975. Secretion of chorion proteins in the follicles of the silkmoth, *A. polyphemus*. Ph. D. Thesis, Harvard University, Cambridge, Mass. 185 pp.
6. CARO, L. G., and R. P. VAN TUBERGEN. 1962. High-resolution autoradiography. 1. Methods. *J. Cell Biol.* **15**:173–188.
7. CASTLE, J. D., J. D. JAMIESON, and G. E. PALADE. 1972. Radioautographic analysis of the secretory process in the parotid acinar cell of the rabbit. *J. Cell Biol.* **53**:290–311.

8. DÖRMER, P., and W. BRINKMANN. 1970. Auflicht-photometric von Mikroautoradiogrammen für quantitative Einbaustudien und Einzelzellen. *Z. Anal. Chem.* **252:**84–89.
9. GRACE, T. D. C. 1962. Establishment of four strains of cells from insect tissues grown *in vitro*. *Nature (Lond.).* **195:**788–798.
10. GRAYSON, S., and S. J. BERRY. 1974. Synthesis and intracellular transport of protein by the colleterial gland of the *Cecropia* silkmoth. *Dev. Biol.* **38:**150–156.
11. GULLBERG, J. E. 1957. A new change-over optical system and direct recording microscope for quantitative autoradiography. *Exp. Cell Res.* **4**(Suppl.)**:**222–234.
12. HOWLING, D. H., and P. J. FITZGERALD. 1959. The nature, significance, and evaluation of the Schwarzschild-Villiger (SV) effect in photometric procedures. *J. Biophys. Biochem. Cytol.* **6:**313–337.
13. JAMIESON, J. D., and G. E. PALADE. 1967. Intracellular transport of secretory proteins in the pancreatic exocrine cell. I. Role of the peripheral elements of the Golgi complex. *J. Cell Biol.* **34:**577–596.
14. JAMIESON, J. D., and G. E. PALADE. 1967. Intracellular transport of secretory proteins in the pancreatic exocrine cell. II. Transport to condensing vacuoles and zymogen granules. *J. Cell Biol.* **34:**597–615.
15. JAMIESON, J. D., and G. E. PALADE. 1971. Synthesis, intracellular transport, and discharge of secretory proteins in stimulated pancreatic exocrine cells. *J. Cell Biol.* **50:**135–158.
16. JAMIESON, J. D., and G. E. PALADE. 1977. Production of secretory proteins in animal cells. *In* International Cell Biology 1976–1977. B. R. Brinkley and K. R. Porter, editors. Rockefeller University Press, New York. 308–317.
17. KAFATOS, F. C., and V. KIORTSIS. 1971. The packaging of a secretory protein: kinetics of cocoonase zymogen transport into a storage vacuole. *J. Cell Biol.* **48:**425–431.
18. KAFATOS, F. C., J. C. REGIER, G. D. MAZUR, M. R. NADEL, H. M. BLAU, W. H. PETRI, A. R. WYMAN, R. E. GELINAS, P. B. MOORE, M. PAUL, A. EFSTRATIADIS, J. N. VOURNAKIS, M. R. GOLDSMITH, J. R. HUNSLEY, B. BAKER, J. NARDI, and M. KOEHLER. 1977. The eggshell of insects: differentiation-specific proteins and the control of their synthesis and accumulation during development. *In* Results and Problems in Cell Differentiation. Vol. 8: Biochemical Differentiation of Insect Glands. W. Beermann, editor. Springer-Verlag, Berlin. 44–145.
19. KOPRIWA, B. M. 1967. The influence of development on the number and appearance of silver grains in electron microscopic radioautography. *J. Histochem. Cytochem.* **15:**501–515.
20. KOPRIWA, B. M. 1967. A semiautomatic instrument for the radioautographic coating technique. *J. Histochem. Cytochem.* **14:**923–929.
21. KRAEHENBUHL, J. P., and J. D. JAMIESON. 1972. Solid phase conjugation of ferritin to Fab-fragments of immunoglobulin G for use in antigen localization on thin sections. *Proc. Natl. Acad. Sci. U.S.A.* **69:**1771–1775.
22. NEELY, J. E., and J. W. COMBS. 1976. Variation in the autoradiographic technique. I. Emulsion-developer combinations assessed by photometric measurement of single silver grains. *J. Histochem. Cytochem.* **24:**1057–1064.
23. NEUTRA, M., and C. P. LEBLOND. 1966. Synthesis of the carbohydrate of mucus in the Golgi complex as shown by electron microscope radioautography of goblet cells from rats injected with glucose-^{3}H. *J. Cell Biol.* **30:**119–136.
24. NEUTRA, M., and C. P. LEBLOND. 1966. Radioautographic comparison of the uptake of galactose-^{3}H and glucose-^{3}H in the Golgi region of various cells secreting glycoproteins or mucopolysaccharides. *J. Cell Biol.* **30:**137–150.
25. PAUL, M., M. R. GOLDSMITH, J. R. HUNSLEY, and F. C. KAFATOS. 1972. Cellular differentiation and specific protein synthesis: production of eggshell proteins by silkmoth follicular cells. *J. Cell Biol.* **55:**653–680.
26. PAUL, M., and F. C. KAFATOS. 1975. Specific protein synthesis in cellular differentiation. II. The program of protein synthetic changes during chorion formation by silkmoth follicles and its implementation in organ culture. *Dev. Biol.* **42:**141–159.
27. REGIER, J. 1975. Silkmoth chorion proteins: rates of synthesis and physical and evolutionary characterization. Ph. D. Thesis. Harvard University, Cambridge, Mass. 116 pp.
28. REVEL, J. P., and E. D. HAY. 1963. An autoradiographic and electron microscopic study of collagen synthesis in differentiating cartilage. *Z. Zellforsch. Mikrosk. Anat.* **61:**110–144.
29. REYNOLDS, C. S. 1963. The use of lead citrate at high pH as an electron-opaque stain in electron microscopy. *J. Cell Biol.* **17:**208–213.
30. ROGERS, A. W. 1961. A simple photometric device for the quantitation of silver grains in autoradiographs of tissue sections. *Exp. Cell Res.* **24:**228–229.
31. ROGERS, A. W. 1967. Techniques in Autoradiography. Elsevier North-Holland, Inc., New York. 335 pp.
32. ROGERS, A. W. 1972. Photometric measurements of grain density in autoradiographs. *J. Microsc. (Oxf.).* **96:**141–153.
33. ROSS, R., and E. P. BENDITT. 1965. Wound healing and collagen formation. *J. Cell Biol.* **27:**83–101.
34. SCHEELE, G. A., and G. E. PALADE. 1975. Studies on the guinea pig pancreas. Parallel discharge of

exocrine enzyme activities. *J. Biol. Chem.* **250:**2660–2670.

35. SMITH, D. S., W. H. TELFER, and A. C. NEVILLE. 1971. Fine structure of the chorion of a moth, *Hyalophora cecropia*. *Tissue Cell.* **3**(3):477–498.
36. TARTAKOFF, A. M., J. D. JAMIESON, G. A. SCHEELE, and G. E. PALADE. 1975. Studies on the pancreas of the guinea pig. Parallel processing and discharge of exocrine proteins. *J. Biol. Chem.* **250:**2671–2677.
37. UHR, J. W. 1970. Intracellular events underlying synthesis and secretion of immunoglobin. *Cell. Immunol.* **1:**228–244.
38. WEIS-FOGH, T. 1970. Structure and formation of insect cuticle. *Symp. R. Entomol. Soc. Lond.* **5:**165–185.
39. WHUR, P., A. HERSCOVICS, and C. P. LEBLOND. 1969. Radioautographic visualization of the incorporation of galactose-^{3}H and mannose-^{3}H by rat thyroids in vitro in relation to the stages of thyroglobulin synthesis. *J. Cell Biol.* **43:**289–311.
40. YUND, M. A., W. F. YUND, and F. C. KAFATOS. 1971. A computer method for analysis of radioactivity data from single and double labeled experiments. *Biochem. Biophys. Res. Commun.* **43:**717–722.